PROCEEDINGS OF SPIE

SPIEDigitalLibrary.org/conference-proceedings-of-spie

Comparative studies of the fluorescence spectroscopy and dynamics of mCerulean3 and mTurquoise2.1 as donors in FRET pairing with mCitrine

Aplin, Cody, Kay, Taryn, Beenken, Julie, Nwachuku, Chioma, Tetteh-Jada, Emmanuel, et al.

Cody P. Aplin, Taryn M. Kay, Julie Beenken, Chioma Nwachuku, Emmanuel Tetteh-Jada, Ahmed A. Heikal, Arnold J. Boersma, Erin D. Sheets, "Comparative studies of the fluorescence spectroscopy and dynamics of mCerulean3 and mTurquoise2.1 as donors in FRET pairing with mCitrine," Proc. SPIE 11497, Ultrafast Nonlinear Imaging and Spectroscopy VIII, 114970T (20 August 2020); doi: 10.1117/12.2571138

SPIE.

Event: SPIE Optical Engineering + Applications, 2020, Online Only

Comparative studies of the fluorescence spectroscopy and dynamics of mCerulean3 and mTurquoise2.1 as donors in FRET pairing with mCitrine

Cody P. Aplin[1], Taryn M. Kay[2], Julie Beenken[1], Chioma Nwachuku[1], Emmanuel Tetteh-Jada[1], Ahmed A. Heikal[1*], Arnold J. Boersma[3*], and Erin D. Sheets[1*]

[1]*Department of Chemistry & Biochemistry,* [2]*Department of Physics and Astronomy, University of Minnesota Duluth, Duluth, MN, 55812 95555-0345*

[3]*DWI-Leibniz Institute for Interactive Materials, Forckenbeckstraße 50, 52056 Aachen, Germany*

* E-mail: aaheikal@d.umn.edu; Phone: 218-726-7036; Fax: 218-726-7394.
* E-mail: edsheets@d.umn.edu; Phone: 218-726-6046; Fax: 218-726-7394.
* E-mail: boersma@dwi.rwth-aachen.de; Phone: 49 241 80-23335.

ABSTRACT

We investigated the donor effects (mCerulean3 *versus* mTurquoise2.1) on the spectroscopy and dynamics of mCerulean3-linker-mCitrine constructs using integrated fluorescence spectroscopy methods. Here, mCerulean3 (a cyan fluorescent protein) and mCitrine (a yellow fluorescent protein) act as Förster resonance energy transfer (FRET) pair, separated by flexible linker region. We hypothesize that the construct with mTurquoise2.1 would have many advantages as a donor, which include a higher FRET efficiency as compared with the mCerulean3 due to the enhanced spectral overlap with mCitrine. To test this hypothesis, we used steady-state spectroscopy, time-resolved fluorescence, and fluorescence correlation spectroscopy of both mCerulean3-linker-mCitrine and mTurquoise2.1-linker-mCitrine to investigate the donor effect on the FRET efficiency and translational diffusion as a means for developing a rational design for hetero-FRET constructs for environmental sensing.

Keywords: FRET, mCerulean3, mTurquoise2.1, mCitrine, time-resolved fluorescence, fluorescence correlation spectroscopy.

1. INTRODUCTION

The interior of living cells is a dynamic, crowded, and complex environment, with a wide range of biomolecules and organelles [1, 2]. Macromolecular crowding in living cells is believed to affect a range of biological processes such as enzyme kinetics, protein-protein interactions, and signaling pathways [3-6]. High levels of crowding have also been attributed to aggregation of amyloid fibrils, which has been observed in patients with Parkinson's and Alzheimer's disease [7-9].

A family of mCerulean3-linker-mCitrine constructs have been developed recently for macromolecular sensing [10]. In these macromolecular crowding sensors, mCerulean3 acts as a donor fluorescent protein and mCitrine acts as an acceptor for Förster resonance energy transfer (FRET), which is considered as a noninvasive molecular ruler to quantify the donor-acceptor distance changes in response to macromolecular crowding. FRET approaches are useful tools for quantitatively measuring a range of biological systems using noninvasive approaches, including protein-DNA complexes [11] and protein conformational dynamics [12]. The energy transfer between a FRET pair is nonradiative and is dependent on the spectral overlap between the emission of the donor and the absorbance of the acceptor, the relative orientation of

Ultrafast Nonlinear Imaging and Spectroscopy VIII, edited by Zhiwen Liu, Demetri Psaltis, Kebin Shi, Proceedings of SPIE Vol. 11497, 114970T · © 2020 SPIE
CCC code: 0277-786X/20/$21 · doi: 10.1117/12.2571138

the transition dipole moment of the donor and the acceptor, the quantum yield of the donor, and the distance between the donor and the acceptor fluorophore [13-17]. Because of the distance dependence of FRET measurements, it has been used as a molecular ruler to measure intermolecular distances between two locations within the cell, each tagged with a fluorophore such as a fluorescent protein or small molecule [18, 19]. FRET can occur between fluorophores of the same species (homo-FRET) or between fluorophores of different species (hetero-FRET), dependent on the spectral overlap of the emission of the donor and the absorbance of the accepting fluorophore [17, 20, 21].

The mCerulean3-mCitrine pair is a good candidate for FRET studies in response to environmental macromolecular crowding due to the separation between the emission of the donor and the emission of the acceptor, the presence of overlap between the emission of the donor and the absorbance of the acceptor, and the high quantum yield (0.87) of the mCerulean3 donor [22]. The macromolecular crowding sensors contain linker regions comprised of a random coil with two electrostatically neutral α-helices, which allow the two fluorescent proteins to be pushed closer together as the level of crowding is increased [10]. This results in a decrease in the donor-acceptor distance and therefore an increase in the measured FRET efficiency.

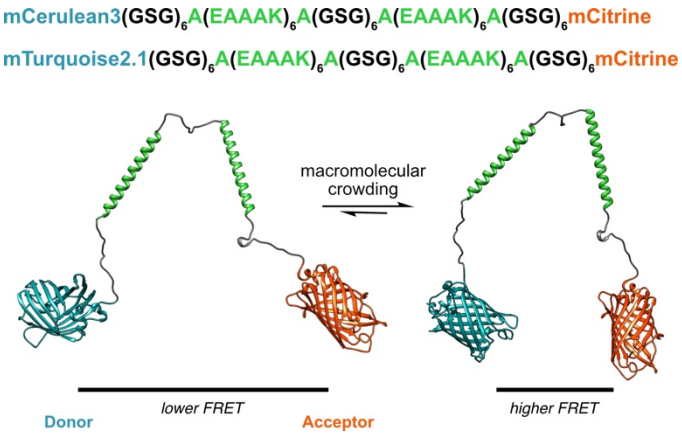

Figure 1: Schematic representation of the molecular structure of mCerulean3-linker-mCitrine along with the amino acid sequences for the linker region. In this construct, the donor (mCerulean3) was replaced by mTurquise2 for comparative studies.

These mCerulean3-linker-mCitrine biosensors have been characterized using a variety of steady-state and time-resolved fluorescence approaches as a function of the amino acid sequences in the linker region. Using time-resolved fluorescence lifetime measurements of mCerulean3, a number of macromolecular crowding sensors (namely, GE, G12, G18, E6, and E6G2) have demonstrated a sensitivity to macromolecular crowding using Ficoll-70 as a crowding agent in a manner that depends on the length and flexibility of the linker region [23]. Additional studies on the rotational dynamics [21] and translational diffusion [24] of these sensors using time-resolved fluorescence anisotropy measurements and fluorescence correlation spectroscopy (FCS), respectively have also been reported. Another family of mCerulean3-linker-mCitrine sensors has been developed for sensing the environmental ionic strength, where the linker region consists of two oppositely charged α-helices [25]. The ionic strength sensors have been previously studied using a time-resolved fluorescence lifetime approach, which demonstrated that these biosensors are sensitivity to the environmental ionic strength using the Hofmeister salt solutions [26].

In this report, we investigated the effect of changing the donor fluorescent protein from mCerulean3 to mTurquoise2.1 in the GE (mCerulean3-linker-mCitrine) sensor for macromolecular crowding. The molecular structure of mCerulean3-linker-mCitrine, referred to as GE(mCer3), and mTurquoise2.1-linker-mCitrine, referred to as GE(mTurq2.1), as representative sensors, is shown in Figure 1. The corresponding amino acid sequence of the flexible linker region is also shown (Figure 1, top). We hypothesize that the higher quantum yield of mTurquoise2.1 will result in a higher FRET efficiency and a larger dynamic range of the FRET sensors. Both proteins contain the identical linker region and acceptor

fluorophore (mCitrine). These protein constructs are investigated using integrated fluorescence approaches including FCS and time-resolved fluorescence measurements of the donor.

2. MATERIALS AND METHODS

2.1 Materials

The protein purification and characterization have been described in detail elsewhere [10, 27]. Briefly, plasmids in the parent pRSET A vector were transformed into the *E. coli* strain and stored at –80 °C as frozen cell stocks [5, 23]. Bacteria were grown in terrific broth that was supplemented with 0.4% (v/v) glycerol and 1.0 $mg.ml^{-1}$ ampicillin until the absorbance at 600 nm reached 0.060 on the NanoDrop2000 spectrophotometer. Protein production was induced with 0.1mM isopropyl-β-D thiogalactoside and incubated for 18 h at 25 °C. The cells were pelleted, resuspended in lysis buffer, and incubated on ice for 30 min [5, 23]. Cells were lysed using probe sonication [5, 23]. Cells were further lysed using an 18.5-gauge needle to draw up the lysate five times, and incubated on ice for 60 min. After centrifuging the cells were lysed to remove cell debris, imidazole was added (10 mM), and the lysate was poured onto a ProBond Ni_2^+–based affinity column that had been previously equilibrated with binding buffer [5, 23]. The column was then washed four times with wash buffer [5, 23]. Protein was eluted with elution buffer into ~1.0 mL fractions [5, 23]. Fractions were dialyzed against phosphate-buffered saline and analyzed using SDS-PAGE to assess purity [5, 23]. A 1:10 dilution of the peak fraction of the construct of interest was used to measure the absorbance spectrum ($\varepsilon \sim 54\,000\ M^{-1}\ cm^{-1}$ at 280 nm) to calculate the concentration.

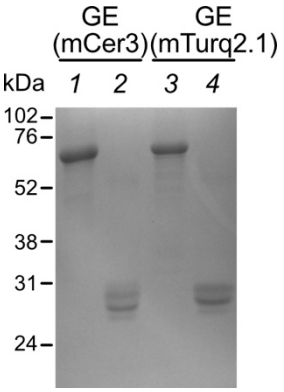

Figure 2: Representative SDS-PAGE of intact (lanes 1 and 3) and cleaved (lanes 2 and 4) GE constructs, GE(mCer3) and GE(mTurq2.1). Only the intact protein is capable of FRET; the cleaved protein is the FRET-incapable control.

Proteinase K was used to cleave the biosensors as a control (Figure 2) experiment as a means to investigate the donor or acceptor alone in the absence of FRET. The fluorescent molecules were diluted in phosphate-buffered saline (PBS, pH 7.4) at ~ 10 nM concentrations.

2.2 Time-Resolved Fluorescence

The experimental setup and data analysis of time-resolved fluorescence measurements have been published in detail elsewhere [23, 26, 28]. Briefly, 425 nm excitation pulses (4.2 MHz, 120 fs) were generated, conditioned, and steered to the back-exit port of an inverted Olympus IX-81 microscope, through a dichroic mirror (396LP), then to the microscope objective lens (1.2NA, Olympus UPlanApo IR, water immersion, 60×) for sample excitation. The fluorescence was filtered (475/50) and detected at the magic angle (54.7°) using a R3809U Hamamatsu multichannel plate photomultiplier tube. The signal was amplified and routed to a synchronized SPC-150N module (Becker & Hickl) for time-correlated single photon counting (TCSPC) detection.

When the fluorescence, $F(t)$,of the intact FRET sensor is excited at 425 nm, the fluorescence of the donor (475/50) can be described by a biexponential model [23, 26]:

$$F(t) = \alpha_1 \, \mathrm{e}^{-(k_{fl}^D + k_{ET})t} + \alpha_2 \, \mathrm{e}^{-k_{fl}^D t} \tag{1}$$

Here, assume that α_1 and α_2 are amplitude fractions ($\alpha_1 + \alpha_2 = 1$) of two distinct subpopulations, one undergoes FRET and fluorescence decay at an overall rate of $\left(k_{ET} + k_{fl}^D\right)$ and the other population decays only via fluorescence (i.e., no FRET) at a rate of $\left(k_{fl}^D\right)$. The average fluorescence lifetime of the donor in the prescence of the acceptor is then given as:

$$\left\langle \tau_{DA} \right\rangle = \frac{\alpha_1 \tau_1 + \alpha_2 \tau_2}{\alpha_1 + \alpha_2} \tag{2}$$

The FRET efficiency of the donor-acceptor pair can then be calculated using the following relationship, where the lifetime of the donor alone is compared to the lifetime of the donor in the presence of the acceptor [27]:

$$E = 1 - \frac{\left\langle \tau_{DA} \right\rangle}{\tau_D} \tag{3}$$

This can in turn to be used to calculate the distance between the donor and the acceptor [29]:

$$R_{DA} = R_0 \cdot \sqrt[6]{\frac{(1-E)}{E}} \tag{4}$$

The acquired time-resolved fluorescence data were analyzed using SPCImage software (Becker & Hickl) and the statistical analysis and figure preparation were conducted using OriginPro software.

2.3 Fluorescence Correlation Spectroscopy

The experimental setup of FCS and the corresponding the fluorescence fluctuation autocorrelation data analysis have been published in detail elsewhere[24, 30]. Briefly, 488-nm laser (cw, Coherent Sapphire 488-20) was used to excite a droplet of the sample (10-30 nM concentration) after a microscope objective (1.2 NA, 60×, water immersion, infinity corrected, Olympus). The collimated fluorescence was then filtered (531/40 nm), focused on a confocal pinhole (50-mm optical fiber), and detected by an avalanche photodiode (APD, SPCM CD-2969, PerkinElmer), and then autocorrelated using external multiple-tau-digital correlator (ALV/6010-160) for data acquisition. Data analysis was carried out using the commercially available OriginPro8 software.

For a molecule undergoing a fluorescence fluctuation due to diffusion only, the three-dimensional (3D), Gaussian autocorrelation function, $G_D(\tau)$, is given by [24, 27, 31]:

$$G_D(\tau) = N^{-1}\left(1 + \tau / \tau_D\right)^{-1}\left(1 + \tau / s^2 \tau_D\right)^{-1/2} \tag{5}$$

Where N is the average number of molecules residing in the open observation volume in the FCS setup, which is characterized by a structure parameter (s). The diffusion time of the molecule (τ_D) is related to its diffusion coefficient according to Stokes-Einstein model, where [24, 27, 31]:

$$\tau_D = \frac{r_{xy}^2}{4D} \tag{6}$$

The lateral (r_{xy}) and axial (r_z) radii of the observation volume are related to the structural parameter, $s = r_z / r_{xy}$. For a molecule undergoing additional i^{th} photophysical process (e.g., intersystem crossing to a triplet state, fluorescence blinking) that takes place on a faster time scale (τ_i) than the corresponding diffusion time (τ_D) during their residency on the observation volume, the corresponding fluorescence fluctuation autocorrelation function, $G_i(\tau)$, is given as an exponential term such that [24, 27, 31]:

$$G_i(\tau) = \left(1 + \frac{f_i}{(1-f_i)} \times e^{-t/\tau_i}\right) \tag{7}$$

Here, a fraction (f_i) of the molecule in the observation volume is assumed to undergo a fast photophysical process such as intersystem crossing to the triplet state (e.g., R110) and fluorescence blinking (e.g., mCitrine).

3. RESULTS AND DISCUSSION

3.1 Steady-State Spectroscopy of the Two Sensors

We investigated the donor effect on the absorption and emission spectra of each GE construct in PBS buffer. The absorption spectra of both GE proteins with mCerulean3 or mTurquoise2.1 (as donors) are shown in Figure 3, where the absorption peaks are normalized with respect to the acceptor (mCitrine) absorption band at 513 nm. The absorption spectrum of the mCerulean3 peaks at 454 nm as compared with the red-shifted absorption of mTurquoise2.1 absorption at 461 nm (Figure 3). These results show that mTurquoise2.1 has a larger extinction coefficient with a slight red shift with respect to that of mCerulean3 in GE(mCer3) construct. This is rather advantageous for future genetically encoded GE in live cell applications, where a slightly longer wavelength can be used for excitation to avoid UV-light induced damage. In addition, the larger extinction coefficient of mTurquoise2.1 in GE(mTurq2.1) would allow for using lower laser intensity for excitation, which would likely to reduce any potential laser-induced photodamage in cell applications.

Figure 3 also shows the emission spectra of GE as a function of the donor (i.e., mCerulean3 *versus* mTurquoise2.1) under different excitation wavelength (425 nm and 490 nm) in order to access the fluorescence emissions of both the donor and acceptor. The results show a red-shifted (8 nm) emission peak of mTurquoise2.1 (480 nm) with respect to the emission peak of mCerulean3 (472 nm). Both donors also exhibit another emission shoulder (peak) at 499 nm (mCerulean3) and 515 nm (mTurquoise2.1), which suggests a larger spectral overlap of the mTurquoise2.1 emission with the acceptor absorption in GE(mTurq2.1) construct. This increase in spectral overlap would likely increase the corresponding FRET efficiency for environmental sensing. As expected, the emission peak (525 nm) of the acceptor (mCitrine) in both versions of GE construct is the same; independent of the donor (Figure 3). There is a potential disadvantage, however, for mTurquoise2.1 as a donor in the GE(mTurq2.1) construct due to the spectral overlap of the donor and acceptor emission (Figure 3) for FRET imaging in multi-channel confocal microscopy.

The steady-state spectroscopy of GE as a function of the donor provides us with the roadmap for our experimental design for time-resolved fluorescence measurements using 425-nm pulsed excitation for FRET analysis (see below). Under those experimental conditions, the emission of the corresponding donor will be detected using 475/50 nm detection filter; both in the presence (intact GE, FRETing) and absence (cleaved GE, non-FRETing) of the acceptor.

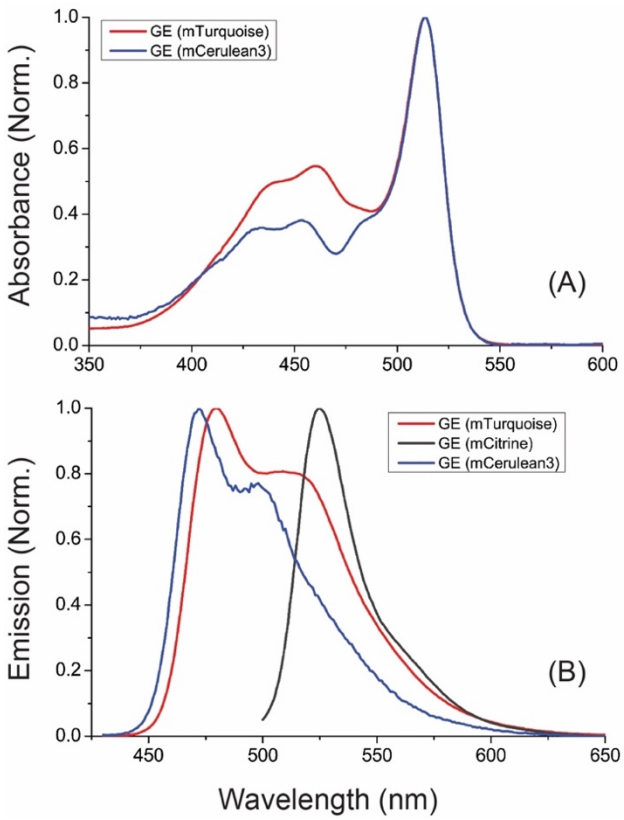

Figure 3: Steady-state spectroscopy of mCerulean3-linker-mCitrine and mTurquoise2.1-linker-mCitrine constructs. (A) The absorption spectra of GE(mTurq2.1) (red curve) and GE(mCer3) (blue curve) in PBS buffer. (B) The emission spectra of GE(mTurq2.1) (red curve) and GE(mCer3) (blue curve) in PBS buffer under 425 nm excitation. Under 490-nm excitation, the emission spectrum of the acceptor (mCitrine; black curve) in both versions of GE is also shown with a fluorescence peak around 525 nm.

3.2 Fluorescence Lifetime of the Donors in the Cleaved and intact Sensors

The excited state lifetime of the mCerulean3 and mTurquoise2.1 were also investigated using 425-nm laser pulses (~120 fs, 4.2 MHz), while the corresponding emission was detected around 475/50 nm. Representative fluorescence decays of intact and cleaved GE are shown in Figure 4 as a function of the donor (i.e., mCerulean3 *versus* mTurquoise2.1).

Our results show that the excited-state fluorescence lifetime of the donor in cleaved GE is consistently longer than that of the intact counterpart, which is attributed to FRET in the presence of the acceptor. The time-resolved fluorescence of the cleaved GE(mCer3) and GE(mTurq2.1) can be described well with a single-exponential decay model with a fluorescence lifetime of 4.08 ns and 3.78 ns, respectively. Under the same experimental conditions, the corresponding time-resolved fluorescence of the intact GE decays as a biexponential with an average fluorescence lifetime of 3.50 ns and 3.81 ns for GE(mCer3) and GE(mTurq2.1), respectively. It is worth mentioning that the fitting of the cleaved GE(mTurq2.1) was a bit better using a biexponential decay model.

We also examined the Ficoll-70 (300 g/L) effect on the excited-state lifetime of GE towards FRET analysis, under the same experimental conditions. Our results indicate that the average fluorescence lifetime of the intact sensor is 3.44 ns for GE(mCer3) as compared with 3.18 ns for GE(mTurq2.1), which reveals macromolecular crowding sensitivity based on the type of the donor in the GE construct. As a control, the fluorescence decays of the cleaved GE proteins were also measured under the same experimental conditions in 300 g/L Ficoll-70. These results were then used to calculate the corresponding FRET efficiency using the average fluorescence lifetime of the cleaved and intact constructs of GE sensor (see below). These fluorescence lifetime results on GE(mCer3) are in general agreement with previous studies [23, 27].

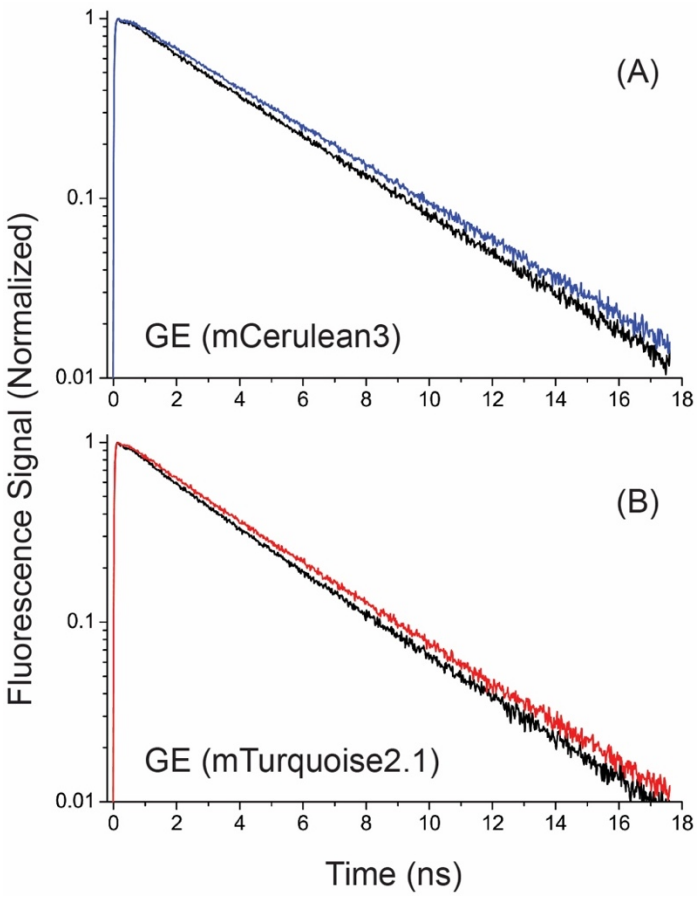

Figure 4: The excited-state fluorescence lifetime of cleaved and intact GE is distinct due to FRET in a buffer. (A) The fluorescence decays of cleaved (blue curve) and intact (black curve) GE with mCerulean3 as a donor. (B) The fluorescence decays of cleaved (blue curve) and intact (black curve) GE with mTurquoise2.1 as a donor. These measurements were carried out using 425-nm pulsed excitation and the fluorescence emission (475/50) of the donor was detected at a magic angle to exclude the rotational dynamics during the excited-state lifetime. The experimental setup was calibrated using coumarin under the same experimental conditions, which has a fluorescence lifetime of 3.83 ns ($\chi^2 = 1.04$).

3.3 Donor-Effect on the FRET Analysis in the Two GE Sensors

Using the measured average fluorescence lifetime of the donor in the presence, $\langle \tau_{DA} \rangle$, and absence, τ_D, of the acceptor in GE constructs, we calculated the corresponding energy transfer efficiency according to equation (3) [27]. The average fluorescence lifetime of the intact, $\langle \tau_{DA} \rangle$ and cleaved, τ_D, GE constructs were measured under the same experimental conditions. The corresponding donor-acceptor distance (R_{DA}) was also calculated using the energy transfer efficiency of each GE construct according to equation (4) [29]. The Förster distance for both GE(mCer3) and GE(mTurq2.1) were assumed to be the same 5.3 nm [10] for simplicity. The results are summarized in Table (2) and Figure 5 below.

Table 1: The FRET efficiency of GE(mCerulean3) and GE(mTurquoise2.1) as calculated using time-resolved fluorescence measurements under 425-nm laser pulses (120 fs, 4.2 MHz). In these measurements, the fluorescence emission of the donor was detected (475/50 nm) in the presence and absence of the acceptor. The donor-acceptor (D-A) distance was also calculated using the corresponding energy transfer efficiency for each GE construct.

Molecule	Environment	FRET Efficiency (%)	D-A Distance (nm)
GE (mCerulean3)	PBS	6.6 ± 0.2	8.2 ± 0.1
	300 g/L Ficoll-70	9.8 ± 0.8	7.8 ± 0.2
GE (mTurquoise2.1)	PBS	7.1 ± 0.5	8.1 ± 0.1
	300 g/L Ficoll-70	11.9 ± 2.0	7.4 ± 0.2

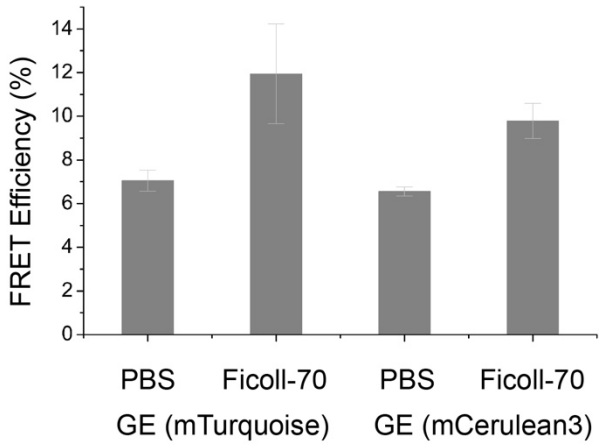

Figure 5: FRET analysis of GE, using time-resolved fluoresce, as a function of the donor and the surrounding environment. The energy transfer efficiency of GE(mTurq2.1) in PBS buffer is slightly larger than that of its counterpart with mCerulean3 as a donor. In addition, the FRET efficiency of GE(mTurq2.1) is more sensitive to the macromolecular crowding of Ficoll-70 (300 g/L) than GE (mCerulean3).

Figure 5 shows a summary of the FRET efficiency of GE constructs (i.e., different donors) in both PBS buffer and Ficoll-70 crowded solution (300 g/L). The results suggest a minor enhancement of the FRET efficiency of GE(mTurq2.1) as compared with GE(mCer3) in PBS buffer at room temperature as well as in Ficoll-70 enriched solution (300 g/L), which support our state hypothesis above. Interestingly, the corresponding donor-acceptor distance in GE(mTurq2.1) is also relatively smaller than that of GE(mCer3) in both PBS buffer and Ficoll-70 solution (Table 1). The FRET analyses of GE(mCer3) are in general agreements with previous studies using the same time-resolved fluorescence approach [23, 27].

3.4 Translational Diffusion Studies of the Two GE Sensors using FCS

Using FCS, we also investigated the fluorescence fluctuation autocorrelation of both GE(mCer3) and GE(mTurq2.1) constructs. As a control, similar measurements were carried out on the cleaved counterpart as well as R110 for the FCS setup calibration. Representative autocorrelation curves of R110 (diffusion coefficient = 4.3 x 10^{-6} cm^2/s [24, 27, 32]) as well as cleaved and intact GE(mTurq2.1) are shown in Figure 6.

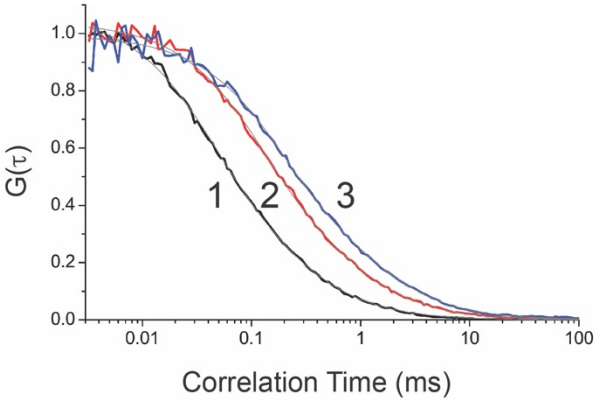

Figure 6: Representative, normalized autocorrelation curves of R110 as well as the cleaved and intact GE(mTurq2.1). The autocorrelation curve of R110 (curve 1), cleaved GE(mTurq2.1) (curve 2), and intact GE(mTurq2.1) (curve 3) are shown. All these autocorrelation curves were measured under 488-nm excitation laser (cw) while the acceptor (mCitrine) emission was detected at 531 nm. Similar measurements were carried out on GE(mCer3) (see Table 2).

Table 2: A summary of the fluorescence fluctuation analysis of the cleaved and intact GE(mCer3) and GE(mTurq2.1) under 488-nm excitation of the acceptor (mCitrine) in a buffer at room temperature. Under the same experimental conditions, the corresponding autocorrelation analyses of R110 are also shown. The calculated diffusion coefficient and hydrodynamic radius of these molecules are also shown. Please notice that the measured molecular brightness shown here may vary under different laser-intensity. The standard deviation of the last digit is shown in parenthesis.

Molecule	Diffusion Time (ms)	Diffusion Coefficient (cm^2/s)	Hydrodynamic Radius (nm)	Molecular Brightness (photon/molecule)
R110	0.13(2)	4.3×10^{-6}	0.56	$2.9(3) \times 10^{3}$
GE(mCer3): Cleaved	0.46(7)	$1.2(4) \times 10^{-6}$	2.0(7)	$1.5(3) \times 10^{3}$
GE(mCer3): Intact	0.67(6)	$8.5(4) \times 10^{-7}$	2.9(2)	$1.7(2) \times 10^{3}$
GE(mTurq2.1): Cleaved	0.41(4)	$1.4(5) \times 10^{-6}$	1.7(6)	$1.8(3) \times 10^{3}$
GE(mTurq2.1): Intact	0.7(1)	$7.9(2) \times 10^{-7}$	3.1(8)	$1.8(3) \times 10^{3}$

Based on the fitting parameters of these autocorrelation curves, the diffusion coefficient, molecular brightness, and the hydrodynamic radius of these molecules were calculated as summarized in Table 2. It is worth mentioning that the autocorrelation curves are best fit by including a fast component of the autocorrelation function that is attributed to intersystem crossing to the triplet state for R110 and fluorescence blinking for the intact and cleaved GE sensors. The estimated diffusion coefficient and hydrodynamic radius of GE(mCer3) are in general agreement with previous studies using the same experimental approach [24, 27]. The diffusion coefficient and hydrodynamic radius of the cleaved GE(mCer3) and GE(mTurq2.1) constructs are about the same and within the stated standard deviation of these measurements. Our results also show that the diffusion coefficient of GE(mTurq2.1) is slightly slower than that of GE(mCer3), which is agreement with their molecular mass as shown in Figure 2. The corresponding hydrodynamic radius of an assumed spherical shaped GE(mTurq2.1) is slightly larger than that of the GE(mCer3).

4. CONCLUSIONS

In this contribution, we investigated the steady-state spectroscopy, excited-state fluorescence lifetime, the FRET efficiency, and the translational diffusion of GE sensors, GE(mCerulean3) and GE(mTurquoise2.1). These studies were carried out to guide us towards a rational design for environmental sensing. Our results indicate that mTurquoise2.1 (as a donor) in the GE(mTurquoise2.1) construct may have some advantages as compared with the GE(mCerulean3) protein. For example, the absorption bands of mTurquoise2.1 are slightly red shifted with respect to those of mCerulean3 as a donor. In addition to the enhanced extinction coefficient, this is rather advantageous in live cells studies, when these sensors are genetically encoded in live cells towards mapping out the cellular macromolecular crowding using fluorescence lifetime imaging microscopy (FLIM) with reduced laser-induced photodamage. The observed red-shifted emission of mTurquoise2.1 are likely to increase the FRET efficiency in the GE constructs due to its enhanced spectral overlap with the acceptor (mCetrine). Under 488-nm excitation of the acceptor (mCitrine), the diffusion coefficient of cleaved and intact GE is distinct and within the FCS sensitivity range. However, the diffusion coefficient of GE(mCerulean3) and GE(mTurquoise2.1) seems too close to resolve using FCS. The molecular brightness of GE(mTurquoise2.1) is slightly larger than that of GE(mCerulean3) under 488-nm excitation in PBS buffer. These results using integrated fluorescence spectroscopy methods represent a step forward towards developing a rational design for FRET constructs for environmental sensing.

ACKNOWLEDGEMENTS

We would like to thank Robert Miller and Christin Libal for their technical help and useful discussion during the course of this project. E.D.S. and A.A.H. acknowledge the financial support provided by the University of Minnesota Grant-in-Aid, a Chancellor's Small Grant, the Department of Chemistry and Biochemistry, the Swenson College of Science and Engineering, University of Minnesota Duluth. A.J.B. acknowledges the financial support of the Netherlands Organization for Scientific Research Vidi grant. C.P.A. was supported by teaching fellowships from the Department of Chemistry and Biochemistry, University of Minnesota Duluth. T.M.K. acknowledges the support of Mylan Radulovich Graduate Fellowship as well as the teaching fellowship from the Department of Physics and Astronomy, University of Minnesota Duluth. We further acknowledge the support from the Minnesota Supercomputing Institute (MSI) at the University of Minnesota.

5. REFERENCES

[1] R. J. Ellis, "Macromolecular crowding: obvious but underappreciated," Trends Biochem. Sci., 26, 597-604 (2001).

[2] A. P. Minton, "Confinement as a determinant of macromolecular structure and reactivity," Biophys. J., 63, 1090-1100 (1992).

[3] D. Tsao, A. P. Minton, and N. V. Dokholyan, "A didactic model of macromolecular crowding effects on protein folding," PLoS One, 5, e11936 (2010).

[4] H. X. Zhou, "Influence of crowded cellular environments on protein folding, binding, and oligomerization: biological consequences and potentials of atomistic modeling," FEBS Lett., 587(8), 1053-61 (2013).

[5] J. Ådén, and P. Wittung-Stafshede, "Folding of an unfolded protein by macromolecular crowding *in vitro*," Biochemistry, 53, 2271-2277 (2014).

[6] P. R. ten Wolde, and A. Mugler, "Importance of crowding in signaling, genetic, and metabolic networks," Int. Rev. Cell Mol. Biol., 307, 419-42 (2014).

[7] L. A. Munishkina, E. M. Cooper, V. N. Uversky *et al.*, "The effect of macromolecular crowding on protein aggregation and amyloid fibril formation," J. Mol. Recognit., 17(5), 456-64 (2004).

[8] M. Delarue, G. P. Brittingham, S. Pfeffer *et al.*, "mTORC1 controls phase separation and the biophysical properties of the cytoplasm by tuning crowding," Cell, 174, 338-349 (2018).

[9] C. Li, L. M. Charlton, A. Lakkavaram *et al.*, “Differential dynamical effects of macromolecular crowding on an intrinsically disordered protein and a globular protein: implications for in-cell NMR spectroscopy,” J. Am. Chem. Soc., 130, 6310-1 (2008).

[10] A. J. Boersma, I. S. Zuhorn, and B. Poolman, “A sensor for quantification of macromolecular crowding in living cells,” Nat. Meth., 12, 227-229 (2015).

[11] A. Hillisch, M. Lorenz, and S. Diekmann, “Recent advances in FRET: distance determination in protein–DNA complexes,” Current opinion in structural biology, 11(2), 201-207 (2001).

[12] K. Truong, and M. Ikura, “The use of FRET imaging microscopy to detect protein–protein interactions and protein conformational changes in vivo,” Curr. Opin. Struct. Biol., 11(5), 573-578 (2001).

[13] R. M. Clegg, [Forster resonance energy transfer—FRET: what is it, why do it, and how it’s done] Elsevier Science, 1 (2009).

[14] E. A. Jares-Erijman, and T. M. Jovin, “FRET imaging,” Nature Biotechnol., 21, 1387-1395 (2003).

[15] D. W. Piston, and G. J. Kremers, “Fluorescent protein FRET: The good, the bad and the ugly,” Trends Biochem. Sci., 32(9), 407-414 (2007).

[16] R. Roy, S. Hohng, and T. Ha, “A practical guide to single-molecule FRET,” Nat. Meth., 5, 507-516 (2018).

[17] M. Tramier, T. Piolot, I. Gautier *et al.*, “Homo-FRET versus hetero-FRET to probe homodimers in living cells,” Methods Enzymol., 360, 580-97 (2003).

[18] C. G. dos Remedios, and P. D. Moens, “Fluorescence resonance energy transfer spectroscopy is a reliable "ruler" for measuring structural changes in proteins. Dispelling the problem of the unknown orientation factor,” J. Struct. Biol., 115(2), 175-85 (1995).

[19] L. Stryer, “Fluorescence energy transfer as a spectroscopic ruler,” Annu Rev Biochem, 47, 819-46 (1978).

[20] S. C. Warren, A. Margineanu, M. Katan *et al.*, “Homo-FRET based biosensors and their application to multiplexed imaging of signalling events in live cells,” Int. J. Mol. Sci., 16(7), 14695-716 (2015).

[21] H. Leopold, R. Leighton, J. Schwarz *et al.*, “Crowding effects on energy transfer efficiencies of hetero-FRET probes as measured using time-resolved fluorescence anisotropy,” J. Phys. Chem. B, 123, 379-393 (2019).

[22] M. L. Markwardt, G. J. Kremers, C. A. Kraft *et al.*, “An improved Cerulean fluorescent protein with enhanced brightness and reduced reversible photoswitching,” PLoS One, 6, e17896 (2011).

[23] J. Schwarz, H. Leopold, R. Leighton *et al.*, “Macromolecular crowding effects on energy transfer efficiency and donor-acceptor distance of hetero-FRET sensors using time-resolved fluorescence,” Methods Appl. Fluoresc., 7, 025002 (2019).

[24] H. B. Lee, A. Cong, H. Leopold *et al.*, “Rotational and translational diffusion of size-dependent fluorescent probes in homogeneous and heterogeneous environments,” Phys. Chem. Chem. Phys., 20, 24045-24057 (2018).

[25] B. Liu, B. Poolman, and A. J. Boersma, “Ionic strength sensing in living cells,” ACS Chem. Biol., 12, 2510-2514 (2017).

[26] R. C. Miller, C. P. Aplin, T. M. Kay *et al.*, “FRET Analysis of Ionic Strength Sensors in the Hofmeister Series of Salt Solutions Using Fluorescence Lifetime Measurements,” J. Phys. Chem. B, 124(17), 3447-3458 (2020).

[27] M. Currie, H. Leopold, J. Schwarz *et al.*, “Fluorescence dynamics of a FRET probe designed for crowding studies,” J. Phys. Chem. B, 121, 5688-5698 (2017).

[28] C. P. Aplin, T. M. Kay, R. C. Miller *et al.*, "Integrated fluorescence approach for FRET analysis of environmental sensors." 11122, 111220E.

[29] J. R. Lakowicz, [Principles of Fluorescence Spectroscopy] Springer, New York(2006).

[30] A. A. Heikal, S. T. Hess, G. S. Baird *et al.*, “Molecular spectroscopy and dynamics of intrinsically fluorescent proteins: coral red (dsRed) and yellow (Citrine),” Proc. Natl. Acad. Sci. U.S.A., 97, 11996-12001 (2000).

[31] P. Schwille, S. Kummer, A. A. Heikal *et al.*, “Fluorescence correlation spectroscopy reveals fast optical excitation-driven intramolecular dynamics of yellow fluorescent proteins,” Proc. Natl. Acad. Sci. U.S.A., 97, 151-156 (2000).

[32] P.-O. Gendron, F. Avaltroni, and K. J. Wilkinson, “Diffusion coefficients of several rhodamine derivatives as determined by pulsed field gradient–nuclear magnetic resonance and fluorescence correlation spectroscopy,” J. Fluoresc., 18(6), 1093 (2008).